Contents lists available at Science-Gate

International Journal of Advanced and Applied Sciences

Journal homepage: http://www.science-gate.com/IJAAS.html

Analysis of an off-grid self-excited dual wound asynchronous generator for wind power generation

Mohamed Arbi Khlifi [1, 2, *]

[1]Department of Electrical Engineering, Islamic University in Madinah, Madinah, Saudi Arabia
[2]Research Laboratory SIME, University of Tunis, Tunis, Tunisia

ARTICLE INFO

Article history:
Received 29 November 2018
Received in revised form
15 March 2019
Accepted 2 April 2019

Keywords:
Double wound asynchronous generator
Self-excited asynchronous generator
Stand-alone
Voltage regulator
Wind power generation

ABSTRACT

The present paper deals with the modeling and control of Wind Energy Conversion System WECS based on an isolated self-excited mode of double wound asynchronous using an FZEO algorithm. We develop the steady-state model of a double wound self-excited asynchronous generator for stand-alone renewable generation dispenses with the segregating real and imaginary components of the complex impedance of the induction generator. Its main objective is to study the sensitivity of the stator mutual leakage inductance on the modeling of such generator, when we used three versions of dual star induction generator electric models. Steady state performances and characteristics of different configurations are clearly examined and compared. Experimental results of the proposed dual three-phase asynchronous generator drive system show the good performance of the analysis system strategy for steady-state conditions. Detailed simulation and experimental investigation about various performances including loading and unloading characteristic of self-excited dual stator asynchronous generator are also presented in the paper.

1. Introduction

Wind energy conversion systems (WECS) are generally equipped with dual stator asynchronous wind power generators functioning at variable speed. For fixed-pitch turbines operating in partial load, maximum energy capture available in the wind generator can be achieved if the turbine rotor operates on the Optimal Regime Characteristic (ORC) (Slimene et al., 2015a; 2015b). This regime can be obtained by tracking some target variables: the optimal rotational speed, depending proportionally on the wind speed, or the optimal rotor power (Marwa et al., 2014; Khlifi and Alshammari, 2014). Several configurations for variable speed wind energy conversion system based on DTAG are available in the literature. Its main role is keeping the DPAG in the stable part of torque-speed characteristic, and this is achieved by varying the slip energy to feed the resistive load, where the rotor energy changes according to speed variation. The main disadvantage of this configuration is its bad efficiency especially when the slip energy increases to an important value (Al Ahmadi et al., 2019; Singh et al., 2010). Multiphase induction machine drives are mainly related to the high-power and/or high-current applications such as for example in electric ship propulsion, in locomotive traction, in aerospace applications and electric/ hybrid vehicles (Singh et al., 2011).

Electric power systems have largely developed as three phase systems, although high phase order (in excess of three) machine construction and power transmission have been considered for last several years. With the growth of increasingly sophisticated design methods and increased importance of economic, environmental and several other factors, the multi-phase systems are being considered as one of the potential alternatives to conventional three-phase systems. Authors in the literature deal with the dual stator machine with extended rotor common to both stators. In all the three cases, output is three-phase. Recently, two papers have reported on modeling and analysis of six-phase self-excited induction generator (Kheldoun et al., 2012; Khlifi, 2018; Haque, 2009). However, so far as the authors have been able to ascertain, practical applications of multi-phase (comprising of more than the conventional three phases) induction generator in hydropower scheme are still unreported.

* Corresponding Author.
Email Address: me.khlifi@uoh.edu.sa
https://doi.org/10.21833/ijaas.2019.06.006
Corresponding author's ORCID profile:
https://orcid.org/0000-0003-2668-6533

The major drawbacks in the use of self-exited double wound asynchronous generator, (DWAG) are the poor voltage and frequency regulations under prime mover speed and load perturbations (Parsa, 2005; Amimeur et al., 2012). The generated terminal voltage and the output frequency, depend on the excitation capacitance, the dual three-phase induction generator parameters, the electrical passive load and the prime mover speed (Levy 1986; Al Ahmadi et al., 2019; Yazdani et al., 2009; Marwa et al., 2013; Khlifi et al., 2016).

This paper, therefore, discusses a sensitivity of mutual leakage reactance of dual stator winding self-excited induction generator configured to operate as a stand-alone electric energy source in conjunction with a hydro power plant. The generator can also supply two separate three-phase loads, which represents an additional advantage. Last but not least, outputs of the dual three-phase windings can be used. Experimental results include study of self-excitation transients with capacitor bank at each of the two three-phase windings and with only one capacitor bank, loading transients with independent three-phase resistive loads at each of the two three-phase winding sets, and measured steady state characteristics for various load and /or capacitor bank configurations.

The presence of the mutual leakage inductance between the two stars of induction machine is due to the fact their windings share the same slots, and are, therefore, mutually coupled. The mutual leakage coupling has an important effect on the harmonic coupling between the two stator winding sets and depends on the winding pitch and the displacement angle between the two stator winding sets. Nevertheless, there have been studies where the mutual leakage coupling has been neglected.

2. The machine model

Fig. 1 shows per phase equivalent circuit of a dual stator SEIG under resistive load. Where $R_{s1}, R_{s1}, R'_r, X_{s1}, X_{s2}, X_{sm}, X'_r, X_c, R_{ch1}, R_{ch2}$ and g represent the stator 1 and 2 resistance, rotor resistance (referred to stator), stator 1 and 2 leakage reactance, mutual leakage reactance between the two stator, magnetizing reactance, rotor leakage reactance (referred to stator), excitation capacitor reactance, load resistance and the generator slip respectively.

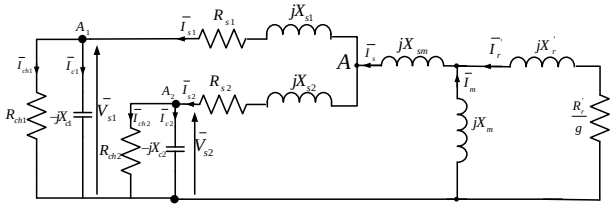

Fig. 1: Equivalent circuit of dual stator self-excited induction generator

When the dual stator SEIG is driven by dc machine in which the shaft speed is maintained constant. All parameters are fixed but both X_m and g vary with the load and hence they must be taken as variables for a given load and excitation capacitance condition. The parameters of the equivalent circuit are given below:

$$\begin{cases} Z_r = \frac{R_r}{g} + jX_r;\ Z_m = jX_m;\ Z_{sm} = jX_m \\ Z_{s1} = R_{s1} + jX_{s1};\ Z_{s2} = R_{s2} + jX_{s2} \\ Z_{c1} = -jX_{c1};\ Z_{c2} = -jX_{C2} \\ Z_{ch1} = R_{ch1} \\ Z_{ch2} = R_{ch2} \end{cases} \quad (1)$$

At note "A" in Fig. 1, the relation between $\bar{I}_{s1}, \bar{I}_{s2}$ and $\bar{I}_s$ can be written as:

$$\bar{I}_s = \bar{I}_{s1} + \bar{I}_{s2} \quad (2)$$

when the two sets of stator three-phase windings are identical, then we can write:

$$\bar{I}_{s1} = \bar{I}_{s2} = \frac{\bar{I}_s}{2} \quad (3)$$

At note "A$_1$" in Fig. 2, the relation between $\bar{I}_{ch1}, \bar{I}_{c1}$ and $\bar{I}_{s1}$ can be written as:

$$\bar{I}_{s1} = \bar{I}_{ch1} + \bar{I}_{c1} \quad (4)$$

where:

$$\begin{vmatrix} I_{C1} \\ I_{ch1} \\ I_{s1} \end{vmatrix} = V_{s1} \begin{vmatrix} Y_{c1} \\ Y_{ch1} \\ -Y_{s1} \end{vmatrix} \quad (5)$$

$$\begin{cases} Y_{c1} = \frac{1}{Z_{c1}} \\ Y_{ch1} = \frac{1}{Z_{ch1}} \\ Y_{s1} = \frac{1}{Z_{s1}} \end{cases} \quad (6)$$

Similarly, the same calculation procedures are adopted to obtain the stator, excitation and load current for the second stator ($\bar{I}_{s2}, \bar{I}_{ch2} + \bar{I}_{c2}$). In order to simplify the study, the following per phase circuit based on impedance analysis are considered, Fig. 2.

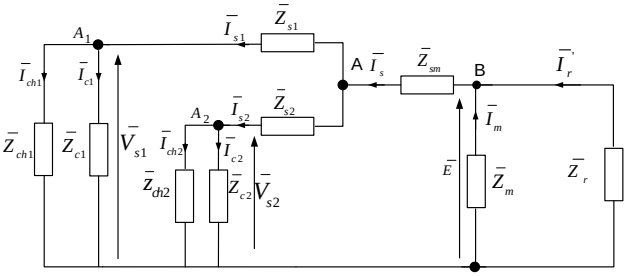

Fig. 2: Simple per phase equivalent circuit of dual stator SEIG

Where, Z_1, Z_2, Y_s, Y_m and Y_r can be represented by using the equivalent circuit as follows:

$$Z_1 = \frac{Z_{ch1}\ Z_{c1}}{Z_{ch1} + Z_{c1}} + Z_{s1} \quad (7)$$

$$Z_2 = \frac{Z_{ch2}\ Z_{c2}}{Z_{ch2} + Z_{c2}} + Z_{s2} \quad (8)$$

$$Y_s = \frac{1}{\frac{Z_1 Z_2}{Z_1 + Z_2} + Z_{sm}} \quad (9)$$

$$Y_m = \frac{1}{Z_m} \quad (10)$$

$$Y_r = \frac{1}{Z_r + \frac{R_r}{g}} \quad (11)$$

At note 'B' in Fig. 2, the relation between I_m, I_r, and I_s can be written as:

$$I_s = I_r + I_m \quad (12)$$

$$\begin{vmatrix} I_m \\ I_r \\ I_s \end{vmatrix} = E \begin{vmatrix} Y_m \\ Y_r \\ Y_s \end{vmatrix} \quad (13)$$

$$\begin{cases} Y_m = \frac{1}{Z_m} \\ Y_r = \frac{1}{Z_r} \\ Y_s = \frac{1}{Z_s} \end{cases} \quad (14)$$

Hence, Eq. 7 can be written as:

$$E(Y_s + Y_m + Y_r) = 0 \quad (15)$$

Under normal operating condition, the stator voltage E≠0 Therefore, the total admittance must be equal to zero.

$$Y_s + Y_m + Y_r = 0 \quad (16)$$

This implies that both the real and imaginary components of Eq. 11 should be independently zero.

$$\begin{cases} \mathrm{Re}(Y_s + Y_m + Y_r) = 0 \\ \mathrm{Im}(Y_s + Y_m + Y_r) = 0 \end{cases} \quad (17)$$

Real (16) and Img (16) is solved by using "fzero" MATLAB function. For a given excitation capacitor and prime mover speed, the system of Eq. 17 has a one unknown parameter, which is the frequency *F*.

Total admittance is considered here as an objective function, and the constrained function is applied to find out simultaneously the value of *F* and X_m. Subsequently, we can predict the necessary parameters to evaluate the performance characteristics of the dual stator SEIG. Flow chart illustrated in Fig. 3, explains the procedure to obtain the desired unknown parameters using the proposed method. The value of *F* and X_m is simultaneously computed for different operating condition by varying the load resistance, and keeping the speed constant at desired value or with fixed excitation capacitance.

3. Results and discussion

The flowchart is given in Fig. 3. Alternatively, the values of star-capacitance at a given speed to generate a particular terminal voltage can be obtained experimentally by using a variable capacitor bank.

Magnetization characteristic of the machine plays an important role in the analysis of dual stator SEIG. These characteristics can be obtained by running the machine at synchronous speed corresponding to line frequency, and measuring the magnetizing inductance for different input voltage at line frequency.

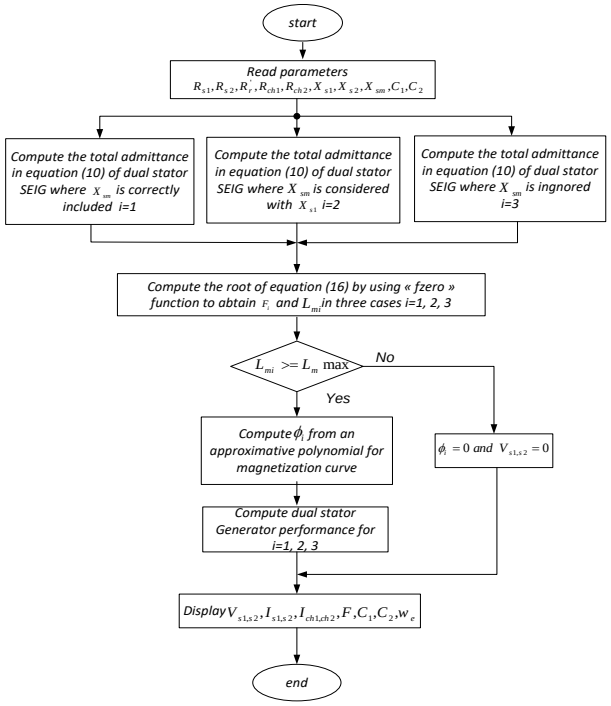

Fig. 3: Flowchart for analysis of dual stator asynchronous generator

The magnetization curve shown in Fig. 4 was approximated by a polynomial of degree 5 as follows:

$$\phi = k_1 L_m^5 + k_2 L_m^4 + k_3 L_m^3 + k_4 L_m^2 + k_5 L_m + k_6 \quad (18)$$

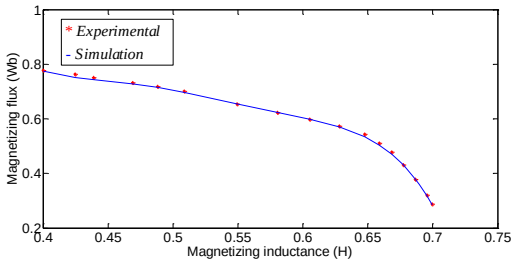

Fig. 4: Magnetization curve of dual stator induction generator

3.1. Impact of the stator mutual leakage inductance in the performances characteristics

The influence of the stator mutual leakage inductance on the electrical performances is less significant. Indeed, if the mutual leakage inductance is neglected compared to the full model, the terminal voltage is about 9%. This variation is about 4.5% if the mutual leakage inductance is included as a self-leakage inductance, Fig. 4. Stator current with speed and self-capacitor presented in Figs. 5 and 6, compared to model 1, is about 2.23% for model 2 and it is around 4.5% for the model 3. In addition, a stator current increase is observed if the mutual leakage inductance is neglected. This allows us to note that performances obtained with model 2, if

mutual leakage is included as a self-inductance, are more acceptable in static mode operation.

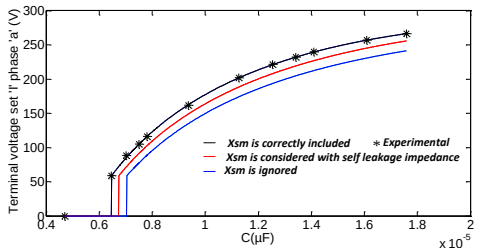

Fig. 5: Terminal voltage with variable capacitance at no load

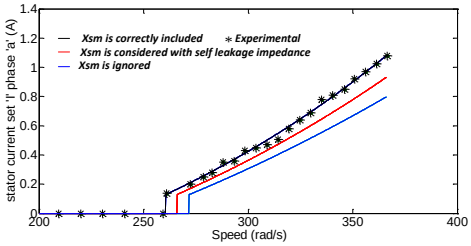

Fig. 6: Stator current with variable speed

To study the sensitivity of such factor, we have considered three possible cases where first the mutual leakage flux is suitably modeled, second it is considered as a self-leakage flux and finally it is totally ignored. The investigation begins with a steady state analysis with experimental validation of dual stator induction generator. The predictions made by model 1 are very close to the experience, it will serve further as a reference in evaluating results obtained with models 2 and 3. This is expected because in model 1, the mutual leakage inductance is correctly introduced. Those made by means of model 3 are the worst (Fig. 7). After writing the adequate set of equations for a dual stator induction generator, the mutual reactance is introduced exactly in the same way as for steady state operation.

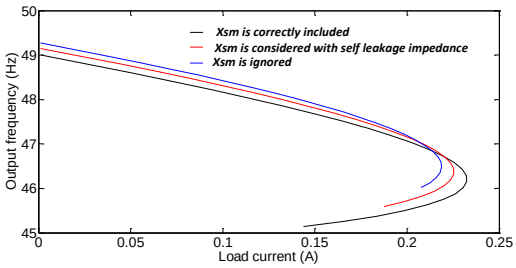

Fig. 7: Output frequency versus load current

3.2. steady state performances characteristics of DWAG

A comparative study will be treated thereafter based on two configuration modes by using simulation and experiments tests.

Nominal configuration: The dual stator SEIG supplied two individual three-phase resistive loads after switching-in a two star connected capacitor bank.

Regulation configuration: the first of the two three-phase stator winding sets is excited and the second is connected at three-phase resistive load.

3.2.1. Nominal configuration

To feed two-independent three-phase loads from dual stator generator, three-phase star connected load banks of variable resistance were connected two each three-phase winding set, Fig. 8.

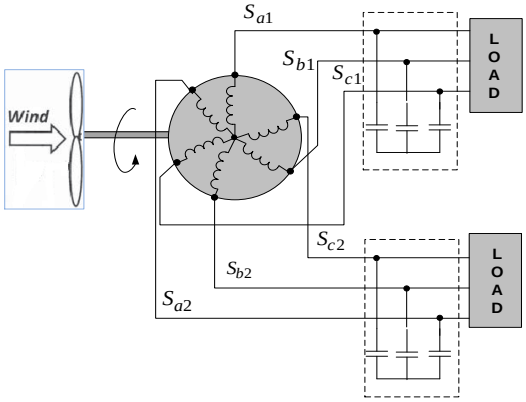

Fig. 8: Scheme of self-excited dual stator winding asynchronous generator

A detailed study of steady-state performance of the dual stator SEIG indicates that for different operating conditions such as change in speed and different values star-capacitance. Self-excitation under no-load condition and loading performance under a typical resistive load are elaborated. For simulation of no-load operation, R_{ch1} and R_{ch2} in the Eq. 1 are replaced by infinity.

The two star-capacitor DSSEIG needs a minimum value of capacitance to self excites at no-load. The no-load terminal voltage can be computed for different value of star-capacitances using a computer algorithm for no-load conditions. Fig. 9 Shows, the behavior obtained from the experiment, of the output voltage as a function of speed. These curves show two areas. The first, when the voltage increases very rapidly with the speed, the corresponding points are those obtained just after the self-excitation. In the second area, voltage varies linearly with the speed to a low coefficient. This area, where the characteristics are substantially parallel, corresponds to the stable part of the dual stator generator.

As depicted in Table 1, with the change in value of excitation capacitance, speed and terminal voltage both change. When the capacity believes, the generator operates more rapidly.

Fig. 10 and Fig. 11 shows the analytical variations of no-load terminal voltage and stator current with excitation capacitance connected to both the double three-phase stator sets at three different speeds.

As shown in Fig. 10, the terminal voltage of the dual stator SEIG increases with increase in the value of the capacitance. However, the saturation of the magnetic circuit of the machine limits the indefinite rise of its terminal voltage. Moreover, the effect of

speed on the stator voltage and corresponding capacitance may also be observed from this Fig. 9. With increase in speed, the capacitance required decreases for a particular voltage, and vice versa. The value of the capacitance at which the machine loses excitation is called the critical capacitance. The value of the critical capacitance is inversely proportional to the square of the speed, therefore the critical square of the speed, therefore the critical capacitance decreases with increase in speed.

Experimental and computed result for variation of terminal voltage and frequency as function of load current are given in Figs. 12 and 13, respectively at three values of capacitor and at rated speed. From Fig. 12, it is observed that there is a rise in load voltage with load when load current varies from 0 to 0.3A, but it starts decreasing when load is further increased.

It is well known that for operation in self-excitation mode, the capacitive excitation is necessary to maintain the machine terminal voltage. If the speed is kept constant at $w_e = 314^{rad}/_{s}$, magnitude of terminal voltage depends on the value of capacitance and the load connected across its terminals. Terminal voltage decreases with the increase in load for a fixed value of capacitance.

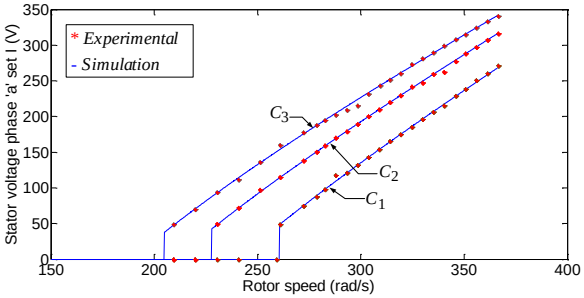

Fig. 9: Output stator voltage versus speed for different values of capacity $C_1 = 9.4\mu F, C_2 = 12.4\mu F, C_3 = 15.4\mu F$

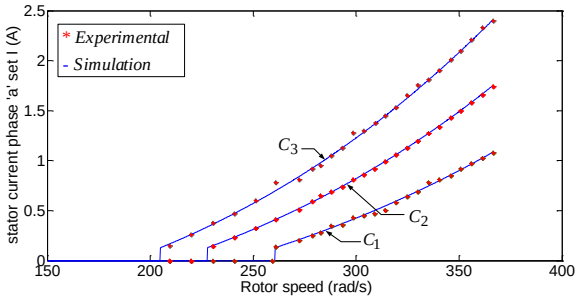

Fig. 10: Stator current versus speed for different values of capacity $C_1 = 9.4\mu F, C_2 = 12.4\mu F, C_3 = 15.4\mu F$

Table 1: Performance evaluation of no-load voltage and current at three values of excitation capacitor

Capacitor bank (μF)	Self-excitation speed $\left(^{rad}/_{s}\right)$	Self-excitation voltage (V)	Self-excitation current (A)	Speed corresponding of nominal voltage current $\left(^{rad}/_{s}\right)$
$C_1 = 9.4$	260.6	48.41	0.128	341.8
$C_2 = 12.4$	227.8	42.43	0.129	314
$C_3 = 15.4$	205.1	40.17	0.13	296.4

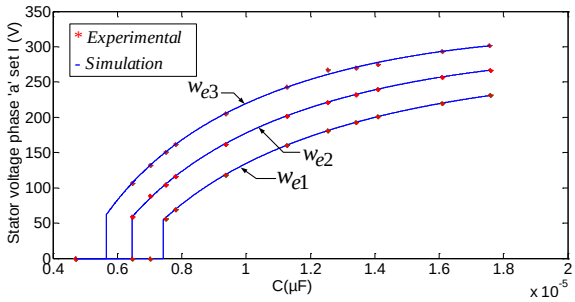

Fig. 11: Variation of terminal voltage with capacitance at no load $w_{e1} = 293^{rad}/_{s}, w_{e2} = 314^{rad}/_{s}, w_{e3} = 335^{rad}/_{s}$

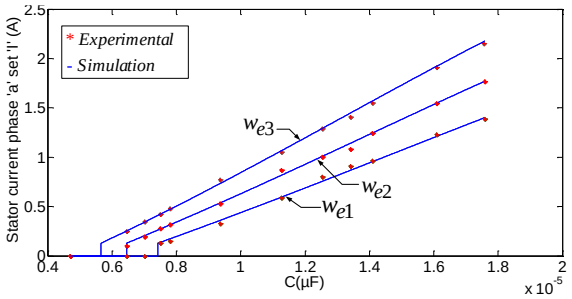

Fig. 12: Variation of stator current with capacitance at no load $w_{e1} = 293^{rad}/_{s}, w_{e2} = 314^{rad}/_{s}, w_{e3} = 335^{rad}/_{s}$

Table 2: Performance evaluation of no-load voltage and current at three speeds

Rotor speed $\left(^{rad}/_{s}\right)$	Self-excitation capacitor (μF)	Self-excitation voltage (V)	Self-excitation current (A)	Capacitor of nominal voltage-current (μF)
$w_{e1} = 293$	7.43	54.58	0.128	16.08
$w_{e2} = 314$	6.46	58.78	0.129	12.44
$w_{e3} = 335$	5.66	62.31	0.31	10.03

Fig. 14 shows the variations of terminal voltage, (across winding set I) with load current when capacitor bank was connected to both the winding sets. Here output is the total power output when both the winding sets were equally supplying a resistive load, the rotor driven at synchronous speed.

Fig. 15 shows the variation of terminal voltage for stator1 versus load current for different values of prime mover speed. The excitation capacitance is fixed at a value of $12\mu F$ and the speed is varied from $293^{rad}/_{s}$ to $335^{rad}/_{s}$ so that for each value of speed the load current is increased gradually up to very high values. Very good agreement between simulation and experimental characteristic is observed.

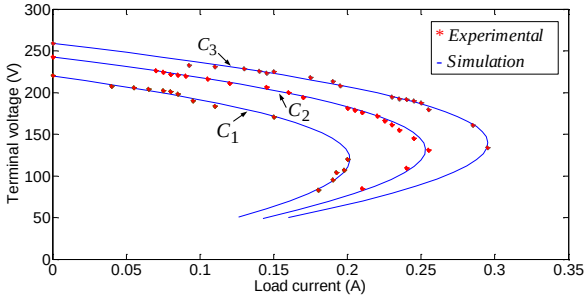

Fig. 13: Terminal voltage for stator 1 with load current at three different capacitor $C_1 = 9.4\mu F$, $C_2 = 12.4\mu F$, $C_3 = 15.4\mu F$

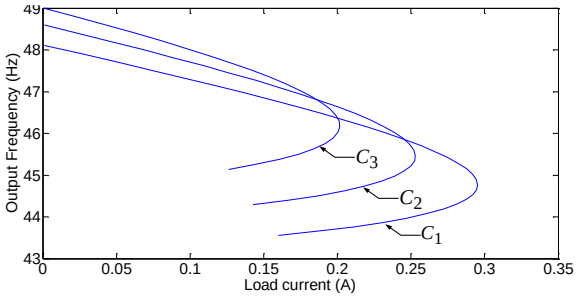

Fig. 14: Output frequency versus load current at three different capacitor $C_1 = 9.4\mu F$, $C_2 = 12.4\mu F$, $C_3 = 15.4\mu F$

Tables 3 and 4 illustrate the comparative performance indices of dual stator SEIG for different value of star capacitance on resistive loading. In this configuration, the double stator SEIG was operating at 1500 rpm.

Table 3: Comparative study of performances of variation of dual stator SEIG in three capacitance configuration

Capacitor bank (μF)	No-load Voltage (V)	Critic Voltage (V)	Critic Load current (A)	Max load current (A)
$C_1 = 9.4$	221	50.34	0.123	0.2
$C_2 = 12.4$	243.2	49.12	0.142	0.255
$C_3 = 15.4$	259.2	49.89	0.159	0.295

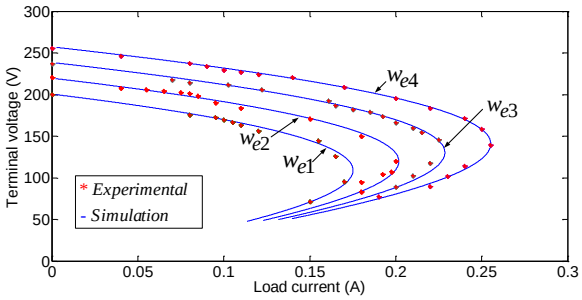

Fig. 15: Terminal voltage for stator 1 with load current $w_{e1} = 293\,^{rad}/_{s}$, $w_{e2} = 314\,^{rad}/_{s}$, $w_{e3} = 335\,^{rad}/_{s}$

Table 4: Comparative study of performances of variation of dual stator SEIG at different speeds

Rotor speed $\left(^{rad}/_{s}\right)$	No-load Voltage (V)	Critic Voltage (V)	Critic Load current(A)	Max load current(A)
$w_{e1} = 293$	200.1	48.56	0.115	0.175
$w_{e2} = 314$	221	50.34	0.123	0.2
$w_{e3} = 324$	237.1	50.31	0.132	0.228
$w_{e4} = 334$	256.6	51.54	0.1411	0.255

3.2.2. Regulation configuration

In this operating mode, only one of three-phase winding set (stator I) was excited and the second three-phase winding set (stator II) are reserved for supplying resistive load. For this purpose, the first stator is considered to be an excitation winding and the second is designed for power and in cases of de-excitation, we excite the second stator to enable the balancing of the operation, so for this reason it is known configuration of regulation, Fig. 16.

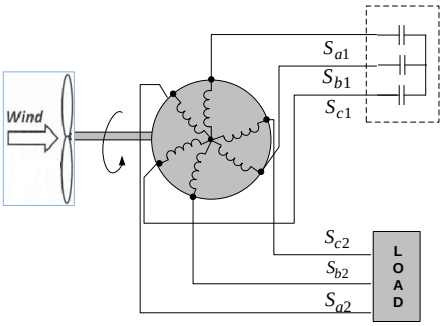

Fig. 16: Scheme of self-regulation of dual stator induction generator

The voltage waveform (at SEIG terminals as well as load terminals) of the two winding sets (stator I and II) for different loading conditions, with excitation at terminals stator I only, were recorded and are given in Fig. 17. It can be observed that loading at any of the two three-phase stator sets affects the voltage of both winding sets. This is an expected consequence of the strong magnetic coupling between the two three- phase stator windings.

The emphasis is placed on additional possibilities offered by using a dual stator SEIG. In particular, it is shown that the dual stator- SEIG can be self-excited without any problems using a single three-phase capacitor bank. This means that, in normal operation, loss of excitation at one of the three-phase windings can be sustained and operation continued (Table 5).

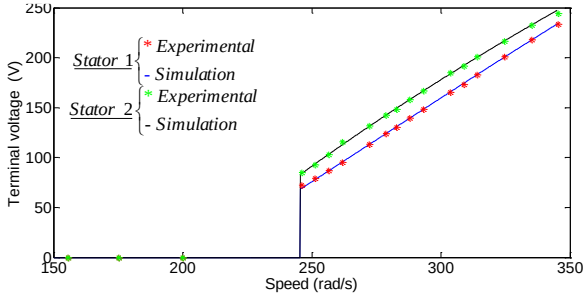

Fig. 17: Terminal voltage for stator I and II

Table 5: Comparative evaluation of no-load terminal voltage of dual stator SEIG against speed when capacitor-bank is connected to stator I

Stator voltage Per phase	Self-excitation speed $\left(rad/_s\right)$	Self-excitation voltage (V)	Speed corresponding of nominal voltage $\left(rad/_s\right)$
V_{as1}	246	72.13	183.1
V_{as2}	246	79.5	195.1

No-load characteristic of dual stator SEIG with C-bank of $C_1 = 22.5$ connected across only one of its three-phase windings (stator I) was also determined. There is a sharp voltage build-up (rise in terminal voltage) across both three-phase winding sets at prime mover speed of $246 rad/s$. When the speed of prime mover is reduced gradually, the voltage collapsed near $155 rad/s$ speed of the prime mover.

Characteristic curves shown in Fig. 15 depict the variation of terminal voltage when second stator winding sets is connected to three phase resistive-load. Terminal voltage of both winding sets starts decreasing with the increase in load.

Time-domain recordings of voltage, given in Fig. 18 clearly show how loading on one winding set affects the voltage and of the other three-phase winding set.

Variable capacitor bank is needed to limit the voltage regulation. When the value of capacitance is too small, it produces negligible capacitive current for magnetization and thus the SEIG cuts off. At the other end, with to large value of capacitance, rotor impedance of the generator causes de-excitation and the voltage collapse again (Table 6).

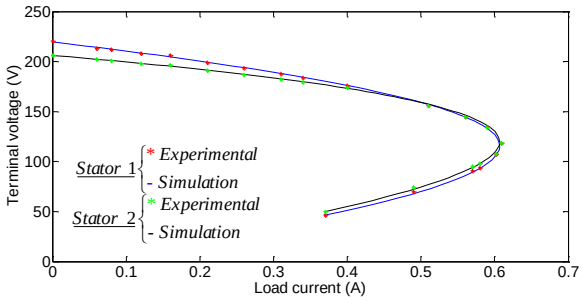

Fig. 18: Load terminal voltage for stator I and II

Table 6: Comparative evaluation of terminal voltage of dual stator SEIG against speed when the second stator is connected to resistive load

Stator voltage per phase	No-load Voltage (V)	Critic Voltage (V)	Critic Load current (A)	Max load current (A)
V_{as1}	220.5	46.45	0.37	0.6
V_{as2}	206.1	50.02	0.37	0.6

4. Conclusion

The paper discusses applicability of double wound asynchronous generator for supplying two individual three-phase loads and for supplying a single three-phase load, by presenting results of a simulation and an experimental study of the steady state behavior for various operating conditions. The sensitivity of the mutual leakage inductance on accuracy of dual stator induction generator models is discussed. Three different models are used to investigate the impact of such parameter, in steady state analysis. It is proven that, if the mutual leakage inductance is not suitably introduced in the modeling process a significant loss of accuracy is resulting. Therefore, models considering that parameter as self-inductance or particularly neglecting it are not recommended, especially in transient operation.

Compliance with ethical standards

Conflict of interest

The authors declare that they have no conflict of interest.

References

Al Ahmadi S, Khlifi MA, and Draou A (2019). Voltage and frequency regulation for autonomous induction generators in small wind power plant. International Journal of Advanced and Applied Sciences, 6(1): 95-98. https://doi.org/10.21833/ijaas.2019.01.013

Amimeur H, Aouzellag D, Abdessemed R, and Ghedamsi K (2012). Sliding mode control of a dual-stator induction generator for wind energy conversion systems. International Journal of Electrical Power and Energy Systems, 42(1): 60-70. https://doi.org/10.1016/j.ijepes.2012.03.024

Haque MH (2009). A novel method of evaluating performance characteristics of a self-excited induction generator. IEEE Transactions on Energy Conversion, 24(2): 358-365. https://doi.org/10.1109/TEC.2009.2016124

Kheldoun A, Refoufi L, and Khodja DE (2012). Analysis of the self-excited induction generator steady state performance using a new efficient algorithm. Electric Power Systems Research, 86: 61-67. https://doi.org/10.1016/j.epsr.2011.12.003

Khlifi MA (2018). Behavior of a dual stator induction machine fed by neutral point clamped multilevel inverter. Journal of Energy, 2018: Article ID 6968023. https://doi.org/10.1155/2018/6968023

Khlifi MA and Alshammari BM (2014). Steady state analysis of an isolated self-excited dual three-phase induction generator for renewable energy. International Journal of Modern Nonlinear Theory and Application, 3(5): 191-198. https://doi.org/10.4236/ijmnta.2014.35021

Khlifi MA, Slimene MB, Fredj MB, and Rhaoulia H (2016). Performance evaluation of self-excited DSIG as a stand-alone distributed energy resources. Electrical Engineering, 98(2): 159-167. https://doi.org/10.1007/s00202-015-0349-y

Levy D (1986). Analysis of a double-stator induction machine used for a variable-speed/constant-frequency small-scale hydro/wind electric power generator. Electric Power Systems

Research, 11(3): 205-223.
https://doi.org/10.1016/0378-7796(86)90035-0

Marwa BS, Mohamed AK, Mouldi BF, and Habib R (2014). Effect of the stator mutual leakage reactance of dual stator induction generator. International Journal of Electrical Energy, 2(3): 1810-1818.

Marwa BS, Mohamed Arbi K, Mouldi B, and Habib R (2013). The process of self-excitation in dual three-phase induction generator. International Review of Electrical Engineering, 8: 1738-1744.

Parsa L (2005). On advantages of multi-phase machines. In the 31st Annual Conference of IEEE Industrial Electronics Society, IEEE, Raleigh, USA.
https://doi.org/10.1109/IECON.2005.1569139

Singh GK, Kumar AS, and Saini RP (2010). A self-excited six-phase induction generator for stand-alone renewable energy generation: Experimental analysis. European Transactions on Electrical Power, 20(7): 884-900.

Singh GK, Kumar AS, and Saini RP (2011). Performance analysis of a simple shunt and series compensated six-phase self-excited induction generator for stand-alone renewable energy generation. Energy Conversion and Management, 52(3): 1688-1699.
https://doi.org/10.1016/j.enconman.2010.10.032

Slimene MB, Khlifi MA, Ben Fredj M, and Rehaoulia H (2015a). Analysis of saturated self-excited dual stator induction generator for wind energy generation. Journal of Circuits, Systems and Computers, 24(9): 1550129.
https://doi.org/10.1142/S0218126615501297

Slimene MB, Khlifi MA, Fredj MB, and Rehaoulia H (2015b). Modeling of a dual stator induction generator with and without cross magnetic saturation. Journal of Magnetics, 20(3): 284-289.
https://doi.org/10.4283/JMAG.2015.20.3.284

Yazdani D, Khajehoddin SA, Bakhshai A, and Joos G (2009). Full utilization of the inverter in split-phase drives by means of a dual three-phase space vector classification algorithm. IEEE Transactions on Industrial Electronics, 56(1): 120-129.
https://doi.org/10.1109/TIE.2008.927405